Modeling Scroll Compressor Performance with Different Refrigerants

Andrew L. HJORTLAND*, Roy R. CRAWFORD[2]

[1]Johnson Controls International plc,
Madison, WI, USA
Email: Andrew.Hjortland@JCI.com

[2]Johnson Controls International plc,
Norman, OK, USA

* Corresponding Author

ABSTRACT

A semi-empirical modeling approach for predicting the flow rate, input power, and discharge temperature of scroll compressors has been developed. Using a dataset comprised of five scroll compressors that were tested with multiple refrigerants, the prediction accuracy of the modeling approach is evaluated. The generalizability of the modeling approach to predict compressor performance of alternative refrigerants is demonstrated. Further refinement of the modeling approach accounting for fluid properties of specific refrigerants is investigated.

1. INTRODUCTION

In the pursuit of improving energy efficiency and reducing greenhouse gas emissions, the heating, ventilation, air conditioning, and refrigeration (HVAC&R) industry is steadily transitioning towards low Global Warming Potential (GWP) refrigerants. This transition poses a significant challenge in compressor technology and HVAC&R system design, particularly in the performance characterization of scroll compressors with these new refrigerants. Scroll compressors, known for their efficiency and reliability in residential and small commercial HVAC&R applications, require a comprehensive understanding of performance metrics such as flow rate, input power, and discharge temperature when operating with a range of refrigerants.

Traditional empirical and fully theoretical models have been used to model compressor performance. However, purely empirical models often fall short in accurately predicting the performance of scroll compressors with untested refrigerants. Moreover, fully theoretical models typically require detailed information that is not available to the system integrator and often require high computational demands. This limitation is particularly pronounced in the early stages of system design, where rapid and reliable performance extrapolation is essential for system optimization.

To address this challenge, a semi-empirical modeling approach that leverages the versatility of empirical modeling while incorporating the predictive strengths of theoretical principles has been developed (Hjortland & Crawford, 2024b). This model is designed to predict some of the key performance indicators of scroll compressors, including: flow rate, input power, and discharge temperature. Using a dataset obtained from five different scroll compressors that were tested with multiple refrigerants, the methodology has been evaluated and compared to the Air-Conditioning, Heating and Refrigeration Institute (AHRI) polynomial modeling approach (Hjortland & Crawford, 2024a).

This paper outlines the development and validation of our semi-empirical model, emphasizing its utility in extrapolating compressor performance to refrigerants not contained in the datasets used to fit the model. Through rigorous evaluation against experimental data, the model's predictive accuracy is demonstrated. Further, enhancements to the model are investigated to improve predictive capability by accounting for specific refrigerant fluid properties.

2. LITERATURE REVIEW

The modeling of compressor performance has evolved significantly over time, with methodologies ranging from simple empirical correlations to complex semi-empirical and theoretical frameworks. At the most basic level, the industry has relied on empirical models, such as the AHRI standard polynomial equations, which predict compressor performance metrics based on coefficients derived from explicit testing with different refrigerants (Air Conditioning, Heating, and Refrigeration Institute, 2020). While straightforward and adequate for refrigerants that have been extensively tested, this approach lacks the flexibility to accurately predict the performance of new or untested refrigerants without undergoing the same extensive testing process.

As the need for more versatile modeling approaches became apparent, especially with the introduction of low GWP refrigerants, researchers began to explore semi-empirical methods. These methods combine empirical data with theoretical principles derived from thermodynamics and fluid mechanics to improve the predictability and generalizability of compressor models. Semi-empirical models often utilize foundational relationships, such as those governing mass flow and energy balances, and incorporate correction factors or functions derived from empirical data. This approach allows for more accurate performance predictions across a wider range of operating conditions and refrigerants, including those not explicitly tested.

Several semi-empirical models have been proposed, each with varying degrees of complexity and applicability. For instance, some models focus on integrating detailed thermodynamic property data of refrigerants into the modeling process, enabling the prediction of compressor performance for a broad spectrum of refrigerants based on their physical and chemical properties (Byrne et al., 2009; Dardenne et al., 2015; Dechesne et al., 2019; Winandy et al., 2002). These advanced semi-empirical models demonstrate significant improvements over purely empirical models, offering a more robust and adaptable framework for predicting compressor performance in the face of changing refrigerant landscapes. Empirical models to predict compressor performance have also been extensively developed (Li, 2012; Marchante-Avellaneda et al., 2023; Navarro-Peris et al., 2013).

The transition from simple empirical models to more sophisticated semi-empirical approaches reflects the HVAC&R industry's ongoing efforts to develop flexible and accurate tools for compressor performance prediction. These advancements not only simplify the design and optimization of systems with known refrigerants but also offer a forward-looking capability to anticipate the performance of scroll compressors with emerging low GWP refrigerants, thereby supporting the industry's move towards sustainability and efficiency.

3. EXPERIMENTAL DATA SOURCES

This study leverages a comprehensive collection of experimental datasets aimed at validating the proposed semi-empirical modeling approach for scroll compressors. These datasets encompass a broad spectrum of testing scenarios, refrigerants, and compressors, providing a robust foundation for assessing the accuracy and generalizability of the model.

A subset of the experimental data was directly collected by the authors through rigorous lab testing. Specifically, Compressor A, a 120.0 $cm^3\ rev^{-1}$ low-side shell scroll compressor designed primarily for medium temperature refrigeration applications, was extensively tested. This compressor, originally qualified for use with refrigerants R-407C and R-134a, was subjected to drop-in system testing with alternative refrigerants R-1234yf, R-516A, and R-1234ze(E) within a reversible air-to-air heat pump system. Key performance indicators such as suction and discharge pressures and temperatures, refrigerant mass flow rate, and compressor electrical measurements were recorded, including a Coriolis flow meter and a multifunction power meter. A variable frequency drive (VFD) was used to adjust the compressor's rotational frequency, enabling the observation of performance across a wide range of operational conditions.

Further data were sourced from the publicly available reports of the Air-Conditioning, Heating, and Refrigeration Institute (AHRI) Low-GWP Alternative Refrigerants Evaluation Program (AREP) (Air-Conditioning, Heating, and Refrigeration Institute, n.d.). This industry-wide initiative focused on identifying and evaluating the potential of low-GWP refrigerants across various compressor applications, including air conditioning and medium-temperature refrigeration. Compressors B–E were tested using a compressor calorimeter setup, adhering to the ANSI/AHRI

Standard 540 (Air-Conditioning, Heating, and Refrigeration Institute, 2004). These tests covered a broad range of operational conditions and were instrumental in evaluating compressor performance with low-GWP refrigerants through drop-in testing. Details of the compressors and refrigerants used in this study are summarized in Table 1.

Table 1: Summary of experimental and literature datasets used for multi-refrigerant modeling validation.

Id.	Source	Test Method	Technology	Refrigerant	Displacement.	Tests
A1	Experimental	System Test	Scroll with Inverter Drive	R-1234ze(E)	120.0 $cm^3\ rev^{-1}$	22
A2	Experimental	System Test	Scroll with Inverter Drive	R-516A[1]	120.0 $cm^3\ rev^{-1}$	45
A3	Experimental	System Test	Scroll with Inverter Drive	R-1234yf	120.0 $cm^3\ rev^{-1}$	54
B1	(Rajendran & Nicholson, 2014d)	Calorimeter	Scroll	R-32	29.5 $cm^3\ rev^{-1}$	23
B2	(Rajendran et al., 2016)	Calorimeter	Scroll	R-454B[2]	29.5 $cm^3\ rev^{-1}$	29
B3	(Rajendran & Nicholson, 2013)	Calorimeter	Scroll	DR-5[3]	29.5 $cm^3\ rev^{-1}$	22
B4	(Rajendran & Nicholson, 2014c)	Calorimeter	Scroll	L-41b[4]	29.5 $cm^3\ rev^{-1}$	30
C1	(Rajendran & Nicholson, 2014a)	Calorimeter	Scroll	R-454A[5]	98.0 $cm^3\ rev^{-1}$	18
C2	(Rajendran & Nicholson, 2014b)	Calorimeter	Scroll	L-40[6]	98.0 $cm^3\ rev^{-1}$	18
D1	(Shrestha, Mahderekal, et al., 2013)	Calorimeter	Scroll	R-410A[7]	20.3 $cm^3\ rev^{-1}$	196
D2	(Shrestha, Mahderekal, et al., 2013)	Calorimeter	Scroll	R-32	20.3 $cm^3\ rev^{-1}$	185
D3	(Shrestha, Mahderekal, et al., 2013)	Calorimeter	Scroll	DR-5[3]	20.3 $cm^3\ rev^{-1}$	192
D4	(Shrestha, Mahderekal, et al., 2013)	Calorimeter	Scroll	L-41a[8]	20.3 $cm^3\ rev^{-1}$	191
E1	(Shrestha, Sharma, et al., 2013)	Calorimeter	Scroll	R-404A[9]	60.0 $cm^3\ rev^{-1}$	190
E2	(Shrestha, Sharma, et al., 2013)	Calorimeter	Scroll	ARM-31a[10]	60.0 $cm^3\ rev^{-1}$	185
E3	(Shrestha, Sharma, et al., 2013)	Calorimeter	Scroll	R-454A[5]	60.0 $cm^3\ rev^{-1}$	182
E4	(Shrestha, Sharma, et al., 2013)	Calorimeter	Scroll	L-40[6]	60.0 $cm^3\ rev^{-1}$	172
E5	(Shrestha, Sharma, et al., 2013)	Calorimeter	Scroll	R-32/R-134a[11]	60.0 $cm^3\ rev^{-1}$	132

[1]R-516A Mass Composition: 77.5% R-1234yf / 8.5% R-134a / 14.0% R-152a
[2]R-454B Mass Composition: 68.9% R-32 / 31.1% R-1234yf
[3]DR-5 Mass Composition: 72.5% R-32 / 27.5% R-1234yf
[4]L-41b Mass Composition: 73% R-32 / 27% R-1234ze(E)
[5]R-454A Mass Composition: 35% R-32 / 65% R-1234yf
[6]L-40 Mass Composition: 40% R-32 / 10% R-152a / 20% R-1234yf / 30% R-1234ze(E)
[7]R-410A Mass Composition: 50.0% R-32 / 50.0% R-125
[8]L-41a Mass Composition: 73% R-32 / 15% R-1234yf / 12% R-1234ze(E)
[9]R-404A Mass Composition: 44.0% R-125 / 52.0% R-143a / 4.0 R-134a
[10]ARM-31a Mass Composition: 28% R-32 / 21% R-134a / 51% R-1234yf
[11]R-32/R-134a Mass Composition: 50% R-32 / 50% R-134a

In total, this work analyzed datasets for five distinct compressors, encompassing eighteen unique combinations of compressors and refrigerants. The selected compressors span a range of applications from comfort heating and cooling to commercial refrigeration, each tested across various suction state conditions, pressure ratios, and, in some cases, variable suction superheats. This comprehensive dataset supports the validation of the semi-empirical modeling approach, providing insights into its applicability and reliability across different refrigerants and operational scenarios. The test conditions for each compressor dataset are summarized in Table 2.

Table 2: Summary of testing ranges of experimental parameters for each dataset.

Id.	Comp. Speed $rev\ s^{-1}$	Suction Pressure MPa (abs)	Suction Superheat K	Pressure Ratio n.d.	Amb. Temperature K
A1	54.00 – 65.00	0.094 – 0.274	2.27 – 15.07	2.90 – 6.57	257.17 – 313.53
A2	45.00 – 60.00	0.142 – 0.401	2.69 – 17.66	2.64 – 6.53	257.11 – 315.07
A3	43.33 – 58.33	0.135 – 0.356	2.86 – 24.49	2.99 – 6.96	256.69 – 314.89
B1	57.28 – 58.98*	0.357 – 1.201	11.11	1.95 – 5.33	308.15
B2	57.50 – 59.32*	0.323 – 1.098	11.11	1.47 – 6.52	308.15
B3	57.62 – 59.23*	0.326 – 0.937	11.11	2.19 – 5.77	308.15
B4	56.80 – 59.35*	0.268 – 0.951	11.11	1.49 – 6.13	308.15
C1	57.82 – 59.35*	0.114 – 0.689	11.11	2.36 – 12.71	308.15
C2	58.43 – 59.40*	0.089 – 0.590	11.11	2.44 – 12.11	308.15
D1	58.33	0.524 – 1.172	5.69 – 30.88	1.59 – 5.14	308.15
D2	58.33	0.538 – 1.200	5.69 – 30.88	1.60 – 4.52	308.15
D3	58.33	0.496 – 1.103	5.69 – 30.88	1.60 – 5.15	308.15
D4	58.33	0.448 – 1.020	5.69 – 30.88	1.62 – 5.19	308.15
E1	58.33	0.264 – 0.633	11.11 – 41.67	2.45 – 8.64	308.15
E2	58.33	0.203 – 0.513	11.11 – 41.67	2.59 – 9.82	308.15
E3	58.33	0.233 – 0.578	11.11 – 41.67	2.54 – 9.24	308.15
E4	58.33	0.195 – 0.501	11.11 – 41.67	2.63 – 8.89	308.15
E5	58.33	0.213 – 0.552	11.11 – 41.67	2.64 – 7.00	308.15

4. METHODOLOGY

The methodology used in this study to model scroll compressor performance utilizes three sub-models based on previous work, each addressing a specific performance metric: flow rate, input power, and discharge temperature (Hjortland & Crawford, 2024b). These models are built on the principles of polytropic compression, which are useful for understanding the behavior of the refrigerants within the compression process.

4.1 Suction Flow Rate Model

The suction flow rate in positive-displacement compressors is fundamentally characterized by the volumetric efficiency, which determines the actual volume of refrigerant drawn into the compression chamber each cycle. The theoretical volumetric flow rate, $\dot{V}_{th}$, is calculated as the product of the compressor's displacement volume, V_{disp}, and its rotational frequency, N,

$$\dot{V}_{th} = V_{disp} \cdot N \tag{1}$$

In practical scenarios, the actual volumetric flow rate, $\dot{V}_s$, deviates from this theoretical value due to factors such as pressure drops, heat transfer, and leakage. These non-ideal influences alter the density of the refrigerant entering the compression chamber, thereby affecting the volumetric efficiency, η_v, defined as,

$$\eta_v = \dot{V}_s / \dot{V}_{th} \tag{2}$$

where $\dot{V}_s$ is the actual volumetric flow rate. Combining Eq. (1) and (2), the actual volumetric flow rate adjusted for non-ideal conditions is expressed through the relationship,

$$\dot{V}_s = \eta_v \cdot V_{disp} \cdot N \tag{3}$$

To account for non-ideal effects, Hjortland and Crawford (2024b) proposed a linear model to predict the volumetric flow rate based on the pressure ratio (p_d/p_s) of the compressor through the empirical parameters a_0 and a_1,

$$\dot{V}_s = N \cdot [a_0 + a_1 \cdot (p_d/p_s)] \tag{4}$$

The mass flow rate generated by the compressor can be simply determined by multiplying Eq. (4) by the density of the refrigerant at the compressor suction. This correlation effectively captures the combined effects of pressure differences, thermal exchanges, and mechanical inefficiencies on the volumetric flow rate, providing a basis for predicting actual flow rates under varying operational conditions. Given the weak dependence of these non-ideal factors on the specific properties of the refrigerant, the original model proposed by Hjortland and Crawford (2024b) is adopted directly in this work without modifications. This decision is supported by empirical observation indicating that the deviations from the theoretical flow rate are influenced more by operational conditions than by the chemical or physical characteristics of the refrigerant.

4.2 Input Power Model

The input power model aims to estimate the power requirement of the compressor motor by incorporating the principles of polytropic compression. The minimum power required for a polytropic compression process is defined as follows (Kuehn et al., 1998),

$$\dot{W}_c = \frac{n}{n-1} \cdot \dot{m}_s \cdot p_s \cdot v_s \cdot \left[\left(\frac{p_d}{p_s} \right)^{\frac{n-1}{n}} - 1 \right] \tag{5}$$

This relationship illustrates that the power required for the compression process is fundamentally dependent on the mass flow rate ($\dot{m}_s$), the suction pressure (p_s), the suction specific volume (v_s), the pressure ratio (p_d/p_s), and the polytropic index (n). However, Eq. (5) assumes ideal gas behavior, which may not be representative of practical conditions, especially at high pressures or near phase transitions.

The actual power required by the compressor will be greater than the thermodynamic work calculated from Eq. (5) due to several factors, including motor inefficiencies, mechanical friction, leakages, and pressure drops. To represent the non-ideal behaviors and real operational conditions more accurately, the following empirical correlation has been proposed (Hjortland & Crawford, 2024b),

$$\dot{W}_e = b_0 + \dot{m}_s \cdot p_s \cdot v_s \cdot \left[b_1 + b_2 \cdot \left(\frac{p_d}{p_s} \right)^{b_3} \right] \tag{6}$$

where $\dot{m}_s$ is the predicted mass flow rate using Eq. (4) and b_0, b_1, b_2, and b_3 are empirical parameters determined from test data. This empirical approach to modeling the input power considers the actual conditions and properties of the refrigerant, which influence the compressor's efficiency and power requirements. During the development of the input power model, a bias was observed when the model as used to extrapolate to different refrigerants. After examination of these prediction errors, the following correction factor was applied to improve the extrapolatory performance of the model,

$$\dot{W}_e = \frac{c_v|_{\text{ref}}}{c_v|_{\text{ref,map}}} \cdot \dot{W}_{e,\text{map}} \tag{7}$$

where $c_v|_{\text{ref}}$ is the isochoric specific heat of the actual refrigerant at a reference state, $c_v|_{\text{ref,map}}$ is the isochoric specific heat of the refrigerant used to determine the model parameters at the same reference state, and $\dot{W}_{e,\text{map}}$ is determined using Eq. (6). In this work, the reference state used to determine the isochoric specific heat of each refrigerant was arbitrarily chosen to be saturated vapor at 0 °C. No attempt was made to optimize the reference state chosen in this work.

4.3 Discharge Temperature Model

Using the ideal gas law, $pv = R_s T$, additional polytropic relationships between pressure, volume, and temperature can be derived (Kuehn et al., 1998). When modeling the temperature change of a polytropic process, the relationship between the temperatures and pressures of the fluid can be used,

$$\frac{T_d}{T_s} = \left(\frac{p_d}{p_s} \right)^{(n-1)/n} \tag{8}$$

where T_d and T_s are the absolute temperature of the suction fluid and discharge fluid, respectively. This relationship is derived under the assumption the fluid behaves as an ideal gas and other dissipative or non-ideal behaviors can be neglected.

To account for deviations from the ideal model, Hjortland and Crawford (2024b) propose the following correlation to predict the compressor discharge temperature,

$$T_d = c_0 + T_s \cdot \left[c_1 + c_2 \cdot \left(\frac{p_d}{p_s} \right)^{c_3} \right] \tag{9}$$

where c_0, c_1, c_2, and c_3 are empirical parameters determined from test data.

4.4 Assumptions

The models assume knowledge of the state of refrigerant at the compressor's suction port, including its pressure and temperature (or enthalpy, density, etc.), as well as the discharge pressure. The rotational frequency of the compressor is also required. This can be directly linked to the output frequency of the drive for an inverter-driven compressor or assumed based on the nominal frequency for fixed-speed units. Additionally, the compressor is presumed to operate under steady-state, steady-flow conditions, which simplifies the modeling by focusing solely on key operating points without transient effects.

These models collectively form the basis of our semi-empirical approach. This methodology allows for the efficient evaluation and prediction of compressor performance in a variety of operational scenarios and with different refrigerants, aligning with the goal of assessing and optimizing the use of low GWP refrigerants in HVAC&R systems.

5. RESULTS

The models described in the previous section are implemented in Python (Python Software Foundation, 2024). Fluid thermodynamic properties calculated from measurements of temperature and pressure using REFPROP, Version 10.0 (Lemmon et al., 2018). The parameters of the models are identified by minimizing the sum of squared errors between measured and calculated quantities (suction mass flow rate, input power, and discharge temperature) for each compressor using one of the refrigerants tested. Using these fitted parameters, the models were then used to predict the compressor performance for the other refrigerants tested to evaluate the extrapolatory performance of the underlying models.

5.1 Mass Flow Rate Modeling Results

The mass flow rate prediction errors are reported for each compressor dataset in Table 3. When the model is applied to the dataset used to fit the model parameters, the observed mean absolute percentage errors (MAPE) of all five compressors were less than 2%. The suction flow rate prediction errors observed when the model was used to extrapolate to different refrigerants is also shown in Table 3. In comparison to the prediction errors of the datasets used to fit the model parameters, larger prediction errors are observed when the model is required to extrapolate to different fluids. The larger prediction errors were the result of a bias in the model when applied to the refrigerants not contained in the original dataset used to fit the model.

Table 3. Mass flow rate prediction errors for each compressor dataset. RMSE: root mean squared error. MAE: mean absolute error. MaxE: maximum absolute error. MAPE: mean absolute percentage error. Shaded rows indicate dataset used to fit model parameters.

Id.	**Refrigerant**	Bias kg h^{-1}	RMSE kg h^{-1}	MAE kg h^{-1}	MaxE kg h^{-1}	MAPE %
A1	R-1234ze(E)	−0.1	1.7	1.3	4.0	0.5
A2	R-516A	3.9	5.2	4.3	9.7	1.2
A3	R-1234yf	25.6	27.5	25.6	42.4	7.0
B1	R-32	−0.1	1.3	1.1	2.7	1.1
B2	R-454B	4.6	5.2	4.6	9.4	3.5
B3	DR-5	2.7	3.1	2.7	6.0	2.7
B4	L-41b	−0.4	2.1	1.6	6.4	1.5
C1	R-454A	−0.1	4.4	3.6	12.1	1.9
C2	L-40	0.2	1.8	1.4	4.1	1.4
D1	R-410A	−0.1	1.1	0.9	2.7	0.8
D2	R-32	−4.4	4.6	4.4	10.0	5.7
D3	DR-5	−2.6	2.8	2.6	4.9	3.1
D4	L-41a	−1.9	2.3	1.9	4.4	2.5
E1	R-404A	0.1	1.3	1.1	4.4	0.6
E2	ARM-31a	−6.1	6.3	6.1	10.6	5.0
E3	R-454A	−7.8	8.2	7.8	15.1	5.8
E4	L-40	−2.1	2.4	2.1	4.0	2.1
E5	R-32/R-134a	−4.2	4.6	4.2	11.0	3.7

A comparison between the predicted and measured suction flow rates for each refrigerant tested in Compressor D is shown in Figure 1. The model prediction errors are also shown in comparison the measured flow rates for each refrigerant tested in Figure 1. While the prediction error bias can be clearly observed, these errors are relatively small when compared to the measured flow rates. This demonstrates that using the model to extrapolate mass flow rate estimation for different refrigerants is possible at least to a first approximation that is typically required for preliminary system design. Qualitatively similar results were observed for the other compressor data sets.

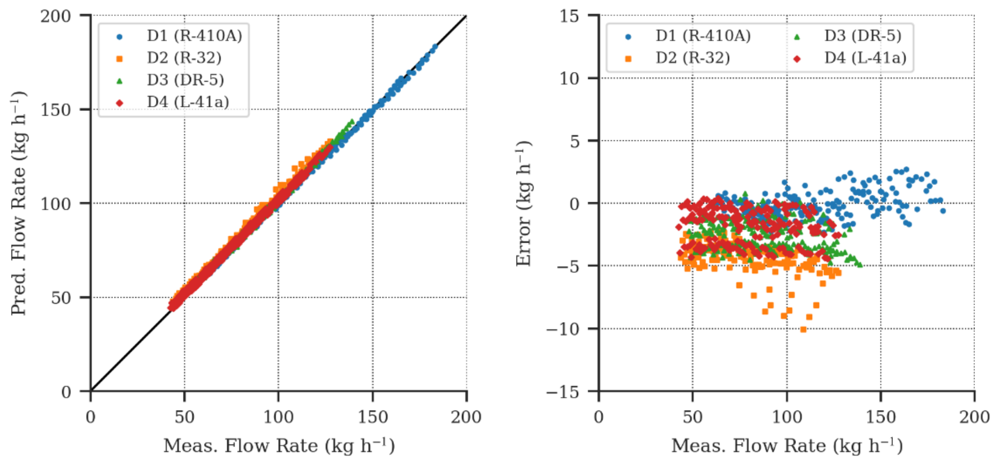

Figure 1. Comparison between measured and predicted flow rates (left) and prediction errors (right) for Compressor D datasets. The model parameters were determined using only dataset D1 and applied to the other data.

5.2 Input Power Modeling Results

The input power prediction errors are reported for each compressor dataset in Table 4. When the model is not required to extrapolate to different refrigerants, the observed MAPE of all five compressors are 1.2% or less. When the model is used to extrapolate the compressor performance with different refrigerants, the observed MAPE are always less than 5.0% and are less than 2.5% in more than half the tested combinations, as shown in Table 4. Like the flow rate prediction, the extrapolated input power predictions were observed to have a bias, which explain the larger prediction errors observed.

Table 4. Input power prediction errors for each compressor dataset. RMSE: root mean squared error. MAE: mean absolute error. MaxE: maximum absolute error. MAPE: mean absolute percentage error. Shaded rows indicate dataset used to fit model parameters.

Id.	**Refrigerant**	Bias W	RMSE W	MAE W	MaxE W	MAPE %
A1	R-1234ze(E)	0.0	31.7	26.3	75.0	0.8
A2	R-516A	−158.9	173.8	158.9	308.2	3.9
A3	R-1234yf	31.3	97.4	85.8	198.5	1.9
B1	R-32	0.0	22.4	16.2	66.0	0.6
B2	R-454B	9.0	78.8	45.5	351.0	2.4
B3	DR-5	−0.1	50.8	42.6	100.6	2.0
B4	L-41b	74.6	80.0	74.6	127.4	3.9
C1	R-454A	0.0	58.6	52.0	100.9	1.2
C2	L-40	69.9	88.8	72.6	168.5	1.9
D1	R-410A	0.0	15.3	11.9	90.2	0.8
D2	R-32	−5.8	30.3	20.0	133.9	1.2
D3	DR-5	−5.9	17.3	13.7	62.7	0.9
D4	L-41a	8.3	16.3	13.5	44.6	1.1
E1	R-404A	0.0	21.5	17.4	63.0	0.6
E2	ARM-31a	−16.3	24.5	20.9	50.1	0.9
E3	R-454A	−43.7	48.3	44.3	77.6	1.7
E4	L-40	−10.7	21.2	18.5	67.9	0.8
E5	R-32/R-134a	139.1	157.3	139.1	379.8	4.9

A comparison between the predicted and measured input for each refrigerant tested in Compressor D is shown in Figure 2. Over the range of operating conditions, the model prediction errors are relatively small, though it can be observed that the model may underpredict the input power at the higher loads. Based on these observations, and the other results reported in Table 4, application of the model to predict the performance of different refrigerants is possible for preliminary system design.

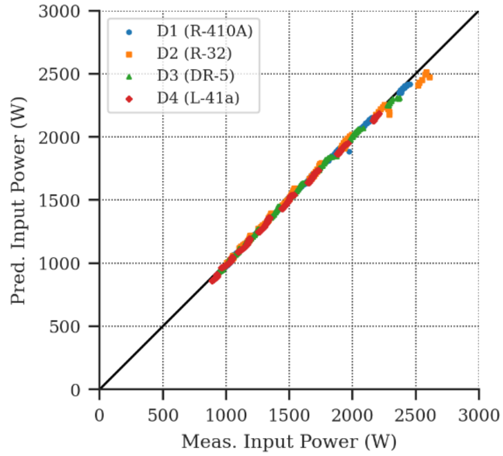

Figure 2. Comparison between measured and predicted input power for Compressor D datasets. The model parameters were determined using only dataset D1 and applied to the other data.

5.3 Discharge Temperature Modeling Results

The discharge temperature prediction errors are reported for each compressor dataset in Table 4. When the model is not required to extrapolate to different refrigerants, the maximum absolute error (MaxE) of all five compressors is less than 5.0 K and the root-mean-squared error (RMSE) is less than 2.0 K. Large prediction errors were observed when the model was used to extrapolate performance to different refrigerants. These errors are the result of large biases present in the extrapolatory predictions of the model. This suggests that differences in thermophysical properties between refrigerants are important for predicting compressor discharge temperatures.

Table 5. Discharge temperature prediction errors for each compressor dataset. RMSE: root mean squared error. MAE: mean absolute error. MaxE: maximum absolute error. Shaded rows indicate dataset used to fit model parameters.

Id.	**Refrigerant**	Bias K	RMSE K	MAE K	MaxE K
A1	R-1234ze(E)	0.0	0.4	0.3	0.8
A2	R-516A	3.9	4.1	3.9	6.4
A3	R-1234yf	−0.5	1.0	0.7	3.1
B1	R-32	0.0	0.6	0.5	1.4
B2	R-454B	−14.0	14.6	14.0	21.9
B3	DR-5	−17.0	17.7	17.0	23.6
B4	L-41b	−13.9	14.9	13.9	21.3
C1	R-454A	0.0	1.9	1.7	3.7
C2	L-40	5.4	5.6	5.4	8.7
D1	R-410A	0.0	1.1	0.8	5.0
D2	R-32	17.8	18.5	17.8	29.5
D3	DR-5	7.4	7.7	7.4	15.8
D4	L-41a	8.0	8.3	8.0	17.5
E1	R-404A	0.0	1.6	1.2	4.3
E2	ARM-31a	9.7	10.0	9.7	19.3
E3	R-454A	12.1	12.4	12.1	24.1
E4	L-40	15.4	15.7	15.4	28.0
E5	R-32/R-134a	25.2	25.7	25.2	39.4

A comparison between the predicted and discharge temperature for each refrigerant tested in Compressor D is shown in Figure 3. Comparing the different prediction accuracy between the different refrigerants, it is clearly observed the model underpredicts the measured value when extrapolation is required. Based on these observations, it is not advisable to use the discharge temperature model when extrapolation to different refrigerants is required. For these cases, other modeling approaches should be developed or pursued.

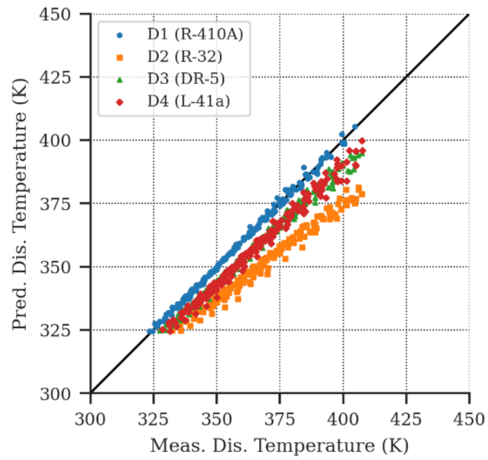

Figure 3. Comparison between measured and predicted discharge temperature for Compressor D datasets. The model parameters were determined using only dataset D1 and applied to the other data. A clear prediction bias is observed when the model is used predict the discharge temperature of different refrigerants.

6. CONCLUSIONS

This study has demonstrated the effectiveness of a semi-empirical modeling approach for predicting the performance of scroll compressors operating with untested refrigerants. The study assessed the extrapolation performance of the prediction of flow rate, input power, and discharge temperature, relying on experimental data from five distinct scroll compressors tested across multiple refrigerants. The semi-empirical model provided acceptable accuracy in predicting the refrigerant flow rate and compressor input power, with the prediction errors being consistently low relative to the observed operational range across different refrigerants. The capability to extrapolate to untested refrigerants was confirmed, although with varying degrees of success, indicating the potential need for model adjustments depending on the specific refrigerant properties. Discharge temperature predictions were less robust when extrapolating to untested refrigerants, suggesting further model development is necessary. This research underscores the importance of developing robust modeling techniques that can adapt to the evolving landscape of refrigerants used in HVAC&R equipment, supporting the industry's ongoing transition towards more sustainable practices.

REFERENCES

Air Conditioning, Heating, and Refrigeration Institute. (2020). *Standard for Performance Rating of Positive Displacement Refrigerant Compressors and Compressor Units*. Air Conditioning, Heating, and Refrigeration Institute. https://www.ahrinet.org/search-standards/ahri-540-si-i-p-performance-rating-positive-displacement-refrigerant-compressors-and-compressor

Air-Conditioning, Heating, and Refrigeration Institute. (n.d.). *AHRI Low-GWP Alternative Refrigerants Evaluation Program*. Retrieved August 22, 2023, from https://www.ahrinet.org/analytics/research/ahri-low-gwp-alternative-refrigerants-evaluation-program

Air-Conditioning, Heating, and Refrigeration Institute. (2004). *ANSI/AHRI 540-2004, Performance Rating of Positive Displacement Refrigerant Compressors and Compressor Units* (Version 2004). Air-Conditioning, Heating, and Refrigeration Institute.

Byrne, P., Miriel, J., & Lenat, Y. (2009). Design and simulation of a heat pump for simultaneous heating and cooling using HFC or CO2 as a working fluid. *International Journal of Refrigeration*, *32*(7), 1711–1723. https://doi.org/10.1016/j.ijrefrig.2009.05.008

Dardenne, L., Fraccari, E., Maggioni, A., Molinaroli, L., Proserpio, L., & Winandy, E. (2015). Semi-empirical modelling of a variable speed scroll compressor with vapour injection. *International Journal of Refrigeration*, *54*, 76–87. https://doi.org/10.1016/j.ijrefrig.2015.03.004

Dechesne, B. J., Tello-Oquendo, F. M., Gendebien, S., & Lemort, V. (2019). Residential air-source heat pump with refrigerant injection and variable speed compressor: Experimental investigation and compressor modeling. *International Journal of Refrigeration*, *108*, 79–90. https://doi.org/10.1016/j.ijrefrig.2019.08.034

Hjortland, A. L., & Crawford, R. R. (2024a). A comparative analysis of a new semi-empirical model and the AHRI polynomial model for positive displacement compressors. *International Journal of Refrigeration*, *159*, 254–263. https://doi.org/10.1016/j.ijrefrig.2023.12.009

Hjortland, A. L., & Crawford, R. R. (2024b). Simplified steady-state modeling of positive displacement compressors. *International Journal of Refrigeration*, *159*, 333–343. https://doi.org/10.1016/j.ijrefrig.2023.12.038

Kuehn, T. H., Ramsey, J. W., & Threlkeld, J. L. (1998). *Thermal Environmental Engineering*. Prentice Hall.

Lemmon, E. W., Bell, I. H., Huber, M. L., & McLinden, M. O. (2018). *NIST Standard Reference Database 23: Reference Fluid Thermodynamic and Transport Properties-REFPROP* (10.0) [Computer software]. National Institute of Standards and Technology. https://doi.org/10.18434/T4/1502528

Li, W. (2012). Simplified steady-state modeling for hermetic compressors with focus on extrapolation. *International Journal of Refrigeration*, *35*(6), 1722–1733. https://doi.org/10.1016/j.ijrefrig.2012.03.008

Marchante-Avellaneda, J., Corberan, J. M., Navarro-Peris, E., & Shrestha, S. S. (2023). A critical analysis of the AHRI polynomials for scroll compressor characterization. *Applied Thermal Engineering*, *219*, 119432. https://doi.org/10.1016/j.applthermaleng.2022.119432

Navarro-Peris, E., Corberán, J. M., Falco, L., & Martínez-Galván, I. O. (2013). New non-dimensional performance parameters for the characterization of refrigeration compressors. *International Journal of Refrigeration*, *36*(7), 1951–1964. https://doi.org/10.1016/j.ijrefrig.2013.07.007

Python Software Foundation. (2024). *Python Language Reference, version 3.12.* [Computer software]. https://www.python.org

Rajendran, R., & Nicholson, A. (2013). *Compressor Calorimeter Test of Refrigerant DR-5 in a R-410A Scroll Compressor* (Test Report #24; AHRI Low-GWP Alternative Refrigerants Evaluation Program (Low-GWP AREP)). Air-Conditioning, Heating, and Refrigeration Institute. https://www.ahrinet.org/system/files/2023-06/AHRI%20Low-GWP%20AREP-Rpt-024.pdf

Rajendran, R., & Nicholson, A. (2014a). *Compressor Calorimeter Test of Refrigerant DR-7 in a R-404A Scroll Compressor* (Test Report #34; AHRI Low-GWP Alternative Refrigerants Evaluation Program (Low-GWP AREP)). Air-Conditioning, Heating, and Refrigeration Institute. https://www.ahrinet.org/system/files/2023-06/AHRI_Low-GWP_AREP-Rpt-034.pdf

Rajendran, R., & Nicholson, A. (2014b). *Compressor Calorimeter Test of Refrigerant L-40 in a R-404A Scroll Compressor* (Test Report #36; AHRI Low-GWP Alternative Refrigerants Evaluation Program (Low-GWP AREP)). Air-Conditioning, Heating, and Refrigeration Institute. https://www.ahrinet.org/system/files/2023-06/AHRI_Low-GWP_AREP-Rpt-036.pdf

Rajendran, R., & Nicholson, A. (2014c). *Compressor Calorimeter Test of Refrigerant L-41b in a R-410A Scroll Compressor* (Test Report #38; AHRI Low-GWP Alternative Refrigerants Evaluation Program (Low-GWP AREP)). Air-Conditioning, Heating, and Refrigeration Institute. https://www.ahrinet.org/system/files/2023-06/AHRI_Low-GWP_AREP-Rpt-038.pdf

Rajendran, R., & Nicholson, A. (2014d). *Compressor Calorimeter Test of Refrigerant R-32 in a R-410A Scroll Compressor* (Test Report #39; AHRI Low-GWP Alternative Refrigerants Evaluation Program (Low-GWP AREP)). Air-Conditioning, Heating, and Refrigeration Institute. https://www.ahrinet.org/system/files/2023-06/AHRI_Low-GWP_AREP-Rpt-039.pdf

Rajendran, R., Pham, H., Bella, B., & Skillen, T. (2016). *Compressor Calorimeter Test of Refrigerant DR-5A in a R-410A Scroll Compressor* (Test Report #58; AHRI Low-GWP Alternative Refrigerants Evaluation Program (Low-GWP AREP)). Air-Conditioning, Heating, and Refrigeration Institute. https://www.ahrinet.org/system/files/2023-06/AHRI_Low_GWP_AREP_Rpt_058.pdf

Shrestha, S., Mahderekal, I., Sharma, V., & Abdelaziz, O. (2013). *Compressor Calorimeter Test of R-410A Alternatives R-32, DR-5, and L-41a* (Test Report #11; AHRI Low-GWP Alternative Refrigerants Evaluation Program (Low-GWP AREP)). Air-Conditioning, Heating, and Refrigeration Institute. https://www.ahrinet.org/system/files/2023-06/AHRI%20Low-GWP%20AREP-Rpt-011.pdf

Shrestha, S., Sharma, V., & Abdelaziz, O. (2013). *Compressor Calorimeter Test of R-404A Alternatives ARM-31a, D2Y-65, L-40, and R-32/R-134a (50/50)* (Test Report #21; AHRI Low-GWP Alternative Refrigerants Evaluation Program (Low-GWP AREP)). Air-Conditioning, Heating, and Refrigeration Institute. https://www.ahrinet.org/system/files/2023-06/AHRI%20Low-GWP%20AREP-Rpt-021.pdf

Winandy, E., Saavedra O., C., & Lebrun, J. (2002). Experimental analysis and simplified modelling of a hermetic scroll refrigeration compressor. *Applied Thermal Engineering*, *22*(2), 107–120. https://doi.org/10.1016/S1359-4311(01)00083-7